Cross-Correlation Tomography: Measuring Dark Energy Evolution with Weak Lensing

Bhuvnesh Jain[1] and Andy Taylor[2]

[1]*Department of Physics and Astronomy, University of Pennsylvania, Philadelphia, Pennsylvania 19104, USA*
[2]*Institute for Astronomy, Royal Observatory, Blackford Hill, Edinburgh EH9 3HJ, United Kingdom*

(Received 10 June 2003; published 3 October 2003)

A cross-correlation technique of lensing tomography is developed to probe dark energy in the Universe. The variation of weak shear with redshift around foreground galaxies depends only on the angular distances and is robust to the dominant systematic error in lensing. We estimate the marginalized accuracies that deep lensing surveys with photometric redshifts can provide on the dark energy density $\Omega_{\rm de}$, the equation of state parameter w, and its evolution w': $\sigma(w) \simeq 0.01 f_{\rm sky}^{-1/2}$ and $\sigma(w') \simeq 0.03 f_{\rm sky}^{-1/2}$, where a prior of $\sigma(\Omega_{\rm de}) = 0.03$ is assumed in the marginalization.

DOI: 10.1103/PhysRevLett.91.141302 PACS numbers: 98.80.Es, 98.62.Sb

Introduction.—Gravitational lensing provides us with the most direct method for probing the distribution of matter in the Universe [1]. Lensing leads to a shear distortion of background galaxy images or a change in the surface number density of background galaxies due to magnification. The measurement of the mass distribution in clusters of galaxies using lensing shear [2,3] and magnification [4–7] are now well established, while on larger scales detections of the cosmic shear signal [8] show that the cosmological matter distribution can also be probed.

The variation of the lensing signal for background galaxies at different redshifts probes the projected lensing mass with different redshift weights in a way that depends on cosmology [9–12]. Hu [12–14] has developed techniques for using the shear power spectrum for background galaxies with photometric redshift information to constrain cosmological parameters, in particular, the nature and evolution of dark energy. His and other recent studies [15–20] have forecast the accuracy with which these parameters can be obtained from future weak lensing surveys, while [21,22] have developed methods to use tomography for 3D mass reconstruction. Observationally weak lensing tomography has been applied to a galaxy cluster [23], but further progress awaits surveys with photometric redshifts of background galaxies.

The lensing shear (or magnification bias) can be used to cross correlate large foreground galaxies (associated with the lensing mass) with background galaxies which are lensed. In this Letter, we will use cross correlations as an alternative way of doing lensing tomography. We use a particularly simple cross-correlation statistic: the average tangential shear around massive foreground halos associated with galaxy groups and galaxy clusters. We show that cross-correlation tomography measures ratios of angular diameter distances over a range of redshifts. Distances are given by integrals of the expansion rate which in turn depends on the equation of state of the dark energy. Thus, the lensing tomography we propose can constrain the evolution of dark energy. We estimate the accuracy with which dark energy parameters can be measured from future lensing surveys.

Formalism.—We work with the metric

$$ds^2 = a^2[-(1+2\phi)d\tau^2 + (1-2\phi)(d\chi^2 + r^2 d\Omega^2)], \tag{1}$$

where we have used the comoving coordinate χ, and $a(\tau) = (1+z)^{-1}$ is the scale factor as a function of conformal time τ. We adopt units such that $c = 1$. The comoving angular diameter distance $r(\chi)$ depends on the curvature: We assume a spatially flat Universe so that $r(\chi) = \chi$. The density parameter Ω has contributions from mass density $\Omega_{\rm m}$ or dark energy density $\Omega_{\rm de}$, so that $\Omega = \Omega_{\rm m} + \Omega_{\rm de}$. The dark energy has equation of state $p = w\rho$, with $w = -1$ corresponding to a cosmological constant. The Hubble parameter $H(a)$ is

$$H(a) = H_0[\Omega_{\rm m} a^{-3} + \Omega_{\rm de} e^{-3\int_1^a d\ln a'[1+w(a')]}]^{1/2}, \tag{2}$$

where H_0 is the Hubble parameter today. The comoving distance $\chi(a)$ is

$$\chi(a) = \int_a^1 \frac{da'}{a'^2 H(a')}. \tag{3}$$

The lensing convergence is given by the weighted projection of the mass density,

$$\kappa(\hat{\boldsymbol{\phi}}) = \frac{3}{2}\Omega_{\rm m}\int_0^{\chi_0} d\chi\, g(\chi)\frac{\delta(r\hat{\boldsymbol{\phi}}, \chi)}{a}, \tag{4}$$

where the radial weight function $g(\chi)$ can be expressed in terms of $r(\chi)$ and the normalized distribution of background galaxies $W_{\rm b}(\chi)$:

$$g(\chi) = r(\chi)\int_\chi^{\chi_0} \frac{r(\chi'-\chi)}{r(\chi')} W_{\rm b}(\chi')\, d\chi', \tag{5}$$

where χ_0 is the distance to the horizon. For a delta-function distribution of background galaxies at $\chi_{\rm b}$, this reduces to $g(\chi, \chi_{\rm b}) = r(\chi)r(\chi_{\rm b} - \chi)/r(\chi_{\rm b})$.

The lensing induced cross correlation between massive foreground halos, which are traced by galaxies, and the tangential shear with respect to the halo center (denoted γ in this paper) is $\omega_\times(\theta) \equiv \langle \delta n_f(\hat{\boldsymbol{\phi}})\gamma(\hat{\boldsymbol{\phi}}')\rangle$, where $n_{\rm f}(\hat{\boldsymbol{\phi}})$

 © 2003 The American Physical Society

is the number density of foreground galaxies with mean redshift $\langle z_f \rangle$, observed in the direction $\hat{\boldsymbol{\phi}}$ in the sky and $\delta n_f(\hat{\boldsymbol{\phi}}) \equiv [n_f(\hat{\boldsymbol{\phi}}) - \bar{n}_f]/\bar{n}_f$. The angle between directions $\hat{\boldsymbol{\phi}}$ and $\hat{\boldsymbol{\phi}}'$ is θ. The cross correlation is given by [24,25]

$$\omega_\times(\theta) = 6\pi^2\Omega_m \int_0^{\chi_0} d\chi W_f(\chi) \frac{g(\chi, \chi_b)}{a(\chi)} \times \int_0^\infty dk\, k P_{hm}(\chi, k) J_\mu[kr(\chi)\theta], \quad (6)$$

where $P_{hm}(\chi, k)$ is the halo-mass cross-power spectrum, and W_f is the foreground halo redshift distribution. The Bessel function J_μ has subscript $\mu = 2$ for the tangential shear and $\mu = 0$ for the convergence [from the relation $\gamma(\theta) = -\frac{1}{2} d\bar{\kappa}(\theta)/d\ln\theta$, [25]]. The measurement of the mean tangential shear around foreground galaxies is called galaxy-galaxy lensing. We will consider a generalization to galaxy groups and clusters.

If the foreground sample has a narrow redshift distribution centered at $\chi = \chi_f$, then we can take W_f to be a Dirac-delta function and evaluate the integral over χ. All terms except $g(\chi_f, \chi_b)$ are then functions of χ_f, the redshift of the lensing mass. The coupling of the foreground and background distributions is contained solely in $g(\chi_f, \chi_b)$. Hence, if we take the ratio of the cross correlation for two background populations with mean redshifts z_1 and z_2, we get

$$\frac{w_1(\theta)}{w_2(\theta)} = \frac{g_1(\chi_f)}{g_2(\chi_f)}, \quad (7)$$

where w_1, g_1 denote the values of the functions for the background population with mean redshift z_1. In the limit that the background galaxies also have a delta-function distribution, this is simply a ratio of distances

$$\frac{w_1(\theta)}{w_2(\theta)} = \frac{r(\chi_1 - \chi_f)/r(\chi_1)}{r(\chi_2 - \chi_f)/r(\chi_2)}. \quad (8)$$

The above equations show that the change in the cross correlation with background redshift does not depend on the galaxy-mass power spectrum, nor on θ. We can simply use measurements over a range of θ to estimate the distance ratio of Eq. (8) for each pair of foreground-background redshifts. The distance ratio in turn depends on the parameters Ω_{de}, w, and its evolution w'. The assumption of thin redshift slices is a requirement only for the foreground population [since Eq. (7) holds for thick background slices]. A thickness smaller than 0.1 in redshift can be achieved even with photometric redshifts, and should be adequately thin for cosmological purposes.

Results.—A simple way to estimate the signal-to-noise for the cross-correlation approach is to regard the foreground galaxies as providing a template for the shear fields of the background galaxies [26]. For a perfect template (i.e., for high density of foreground galaxies and no biasing), the errors are solely due to the finite intrinsic ellipticities of background galaxies. Thus, the fractional error in our measurement of the background shears is simply

$$\frac{\delta\gamma}{\gamma} \sim \frac{\sigma_\epsilon}{\sqrt{N_{total}}\langle\gamma\rangle_{rms}}. \quad (9)$$

The total number of background galaxies is $N_{total} = n_g A = n_g f_{sky} A_{sky}$, where A is the survey area, the lensing induced rms shear $\langle\gamma\rangle_{rms} \simeq 0.04$ [9], and the intrinsic ellipticity dispersion $\sigma_\epsilon = 0.3$. This gives

$$\frac{\delta\gamma}{\gamma} \sim 0.2 \times 10^{-3} \left(\frac{100}{n_g}\right)^{1/2} \left(\frac{0.1}{f_{sky}}\right)^{1/2}, \quad (10)$$

where the number density n_g has units per square arcminute. For the fiducial parameters $f_{sky} = 0.1$ and $n_g = 100$, one can expect to measure the shear to 0.1% accuracy at about 5-σ. Such a signal corresponds to changes in w of a few percent giving the approximate sensitivity we expect in the absence of systematic errors.

To construct a simple and observationally robust cross-correlation statistic, we restrict the foreground sample to galaxy clusters and large galaxy groups. We use the tangential component of the shear for two background samples at different redshifts, inside apertures of size $\theta_{ap} \sim 3'$, as our estimator of the distance ratio of Eq. (7). The tangential shear around a foreground halo is $\langle\gamma(\theta)\rangle = [\bar{\Sigma}(\theta) - \Sigma(\theta)]/\Sigma_{crit}$, where $\Sigma_{crit} = (c^2/4\pi G)(D_s/D_l D_{ls})$ is the geometrical factor that depends on angular diameter distances. To compute the average shear around halos within a mass range, one replaces the projected mass density Σ by the projection of the halo-mass correlation function, so that the above equation is equivalent to Eq. (6) in the limit of thin redshift distributions. We will assume that the massive foreground halos at $z < 1$ have spectroscopic or accurate photometric redshifts. Each background galaxy has a photometric redshift which may be much less accurate.

To compute the accuracy with which parameters can be measured, we need to know the signal and the noise. The signal is given by Eq. (6) in which the halo-mass cross correlation can be accurately computed using the halo model of large-scale structure (see [27] for a review). The model specifies $n(m, z)$, the comoving number density of halos with mass m, the bias parameter of halos, and the density profile of a halo for given mass and redshift. Details of the model are given in [28,29].

The two key quantities for each redshift bin are the number density of halos and the mean shear for each halo mass. We choose the mass range $4 \times 10^{13} < m/M_\odot < 10^{15}$ and aperture size $\theta_{ap} = 2'$–$5'$ corresponding roughly to the virial radii of halos over the redshift range used. We set a constant inner aperture $\theta = 0.1'$ to exclude the strong lensing regime and the luminous parts of the lensing halos. With foreground redshift slices of width $\Delta z = 0.1$, the halos in each slice cover 1/10 the survey area. Using all the foreground slices over $0 < z_f < 1$, the entire survey area is covered.

We take the background redshift distribution to be given by $dN/dz \sim z^a \exp-(z/z_0)^b$, with $a = 2$, $b = 1.5$, and $z_0 = 1$ giving a mean redshift of 1.5. We normalize it to a total number of density $n_g = 100$ per square arcminute. It is split into two background samples, between z_f and $z = 3.0$, with about half the galaxies in each sample. The halo model is used to obtain the mean shear for each lens-source redshift distribution by summing the contributions of halos over the chosen mass range. Note that the inferred parameter values do not rely on the masses or any other property of the halos.

We perform a χ^2 minimization over the mean shear amplitudes at the two background distributions for each foreground slice for the dark energy parameters. The time dependence of w is parametrized as $w = w_0 + w_a(1 - a)$ [30]. For comparison with other work, we will compare w_a to w' defined by $w = w_0 + w'z$. Since the w' parametrization is unsuitable for the large redshift range we use, any comparison with it can be made only for a choice of redshift. At $z = 1$, which is well probed by our method and is of interest in discriminating dark energy models [30], $w_a = 2w'$. For foreground slices labeled by index l and two background samples by 1 and 2,

$$\chi^2 = \sum_l \left[1 - \frac{R^0(z_l, z_1, z_2)}{R(z_l, z_1, z_2)} \right]^2 U_l, \qquad (11)$$

where R is the distance ratio of Eq. (7) for given values of Ω_{de}, w, and w_a, and R^0 is the fiducial model with $\Omega_{de} = 0.7$, $w = -1$, and $w_a = 0$. The weights U_l are

$$U_l^{-1} = \frac{\sigma_\epsilon^2}{2n_1 f_l A \langle\gamma\rangle_{l1}^2} + \frac{\sigma_\epsilon^2}{2n_2 f_l A \langle\gamma\rangle_{l2}^2}, \qquad (12)$$

where f_l is the fraction of the survey area A covered by halo apertures in the lth lens slice. The factor of 2 in the denominator arises because we are using only one component of the measured ellipticity whereas σ_ϵ^2 denotes the sum of the variances of both components.

The results are shown in Figs. 1 and 2. Figure 1 shows the constraints in the $\Omega_{de} - w$ plane. The ellipses show 68% ($\Delta\chi^2 = 2.3$) confidence limits. The elongated inner contour is for fixed $w_a = 0$. The two outer contours marginalize over w_a with external constraints on Ω_{de} from, e.g., the cosmic microwave background, with $\sigma(\Omega_{de}) = 0.01$, 0.03.

Figure 2 shows the constraints in the $w - w_a$ plane if Ω_{de} is fixed, or marginalized with $\sigma(\Omega_{de}) = 0.01$, 0.03. The corresponding accuracy on w and w' scales as $f_{sky}^{-1/2}$. For the case with $\sigma(\Omega_{de}) = 0.03$, we obtain $\sigma(w) \simeq 0.01 f_{sky}^{-1/2}$ and $\sigma(w_a) \simeq 0.06 f_{sky}^{-1/2}$ (at $z = 1$ this is equivalent to $\sigma(w') \simeq 0.03 f_{sky}^{-1/2}$). Note that the value of σ on a parameter is given by projecting the $\Delta\chi^2 = 1$ contour on the parameter axis. The scaling with f_{sky} in the parameter errors comes from the number of background galaxies. For fixed f_{sky} varying the depth of the survey scales the errors as $n_g^{-1/2}$. The results we have shown are for the fiducial redshift $z = 0$. A different choice of the fiducial redshift changes the relative accuracy on w and w_a because the degeneracy direction in the three parameters changes. A detailed exploration of other models of $w(a)$ with finer bins would be of interest.

Discussion.—We have presented a method of lensing tomography that uses foreground halos associated with the lensing mass to measure angular diameter distances over a range of redshifts, $0 \lesssim z \lesssim 3$. It offers an observationally robust probe of dark energy and its evolution over this redshift range. The accuracy achievable with a lensing survey that covers 1/10 of the sky (with parameters close to that of the survey proposed with the LSST telescope) is better than 5% in w and 10% in its

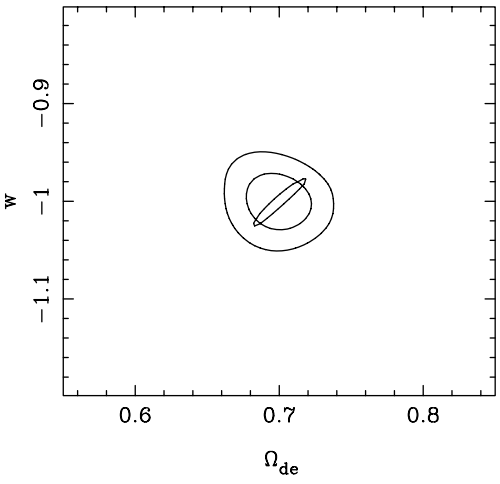

FIG. 1. Contours in the $\Omega_{de} - w$ plane for the fiducial lensing survey with $f_{sky} = 0.1$. The inner contour assumes no evolution of dark energy, $w_a = 0$, while the two outer contours marginalize over w_a, with external constraints on Ω_{de} corresponding to $\sigma(\Omega_{de}) = 0.01$, 0.03 (see text). The 68% confidence interval is shown in each of the contours.

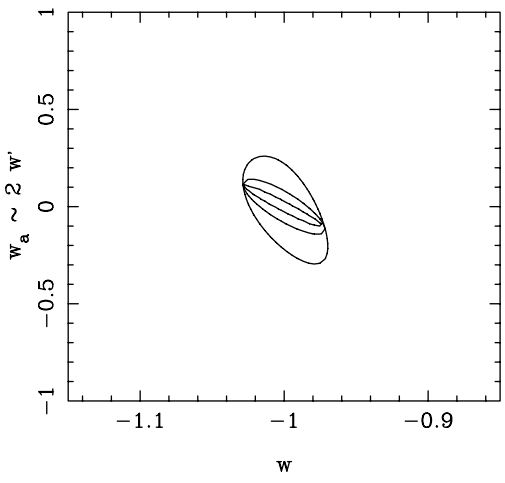

FIG. 2. Contours in the $w - w'$ plane for the fiducial lensing survey with $f_{sky} = 0.1$, as in Fig. 1. The inner contour assumes $\Omega_{de} = 0.7$, while the outer two contours marginalize over Ω_{de} as in Fig. 1. Note that the parameter $w_a = 2w'$ at $z = 1$ (see discussion in the text).

evolution parametrized as w'. This accuracy on the evolution parameter of dark energy is one of the most promising for proposed surveys in the coming decade. It is complementary with constraints from type 1a supernovae in that the redshift coverage is broader while the distance factors probed are similar [20]. Combining cross-correlation tomography with the standard shear power spectrum tomography improves the constraints significantly, since the contour ellipses are oriented differently [14]. Further, it would allow the constraints on the dark matter, such as on neutrino mass, from shear power spectrum tomography to be improved by providing independent information on the geometry.

The practical advantages of cross-correlation tomography are (i) large amplitude shear values ($\sim$ 1–10%) around massive halos are used, and (ii) linear shear amplitudes are compared in the *same* apertures on the sky. The statistic is thus largely insensitive to variation of the point spread function over the field view. The imaging requirements are far less stringent than for standard tomography. The ongoing Canada-France-Hawaii Legacy survey should allow for testing of the method. The limiting systematic error for most surveys is likely to come from the photometric redshifts of the background galaxies. While large statistical errors do not affect the parameter constraints significantly, systematic errors could bias the inferred distance ratios. Calibrating a fair subsample of the photometric redshifts with spectroscopic redshifts, and testing for effects such as possible correlations between measured ellipticities and the sizes or surface brightness of galaxies, should allow us to safeguard against such biases [31].

Our implementation of halo-shear cross correlations is not optimal in that we have used only a fraction of the measured shapes for each lens slice, and only two bins of the background galaxies (motivated by the finding that this provides most of the information in shear power spectrum tomography [12]). The parameter accuracy can therefore be improved with an optimal scheme in which we use the actual redshifts of foreground and background galaxies rather than binning them. It will also be of interest to study different models of $w(z)$ rather than the parametrization used here, or to obtain model independent constraints on the expansion history directly [32,30]. A joint analysis with shear-shear correlations is needed to quantify the improved precision one can expect — this is especially appealing because the two techniques use the data in different regimes, the linear and strongly nonlinear regime, and our technique isolates the dependence on angular diameter distances. We have restricted ourselves to the weak lensing shear; additional information can be obtained by using the strong lensing signal expected in some fraction of the galaxy and cluster halos (for related studies with lensing arcs from galaxy clusters, see [33–35]) and using the magnification signal.

We thank G. Bernstein for many insightful conversations. We thank E. Bertschinger, A. Heavens, W. Hu, M. Jarvis, E. Linder, U. Pen, R. Sheth, and M. Takada for helpful discussions. B. J. is supported by NASA Grant No. NAG5-10923 and a Keck foundation grant. A. N. T. thanks the PPARC for support and the University of Pennsylvania for its hospitality while this work was in development.

[1] Y. Mellier, Annu. Rev. Astron. Astrophys. **37**, 127 (1999); M. Bartelmann and P. Schneider, Phys. Rep. **340**, 291 (2001).
[2] J. A. Tyson, R. A. Wenk, and F. Valdes, Astrophys. J. **349**, L1 (1990).
[3] N. Kaiser and G. Squires, Astrophys. J. **404**, 441 (1993)
[4] J. A. Tyson, Astron. J. **96**, 1 (1998).
[5] T. Broadhurst, A. Taylor, and J. Peacock, Astrophys. J. **438**, 49 (1995).
[6] B. Fort, Y. Mellier, and M. Dantel-Fort, Astron. Astrophys. **321**, 353 (1997).
[7] A. N. Taylor *et al.*, Astrophys. J. **501**, 539 (1998).
[8] D. Bacon, A. Refregier, and R. Ellis, Mon. Not. R. Astron. Soc. **318**, 625 (2000); N. Kaiser, G. Wilson, and G. A. Luppino, astro-ph/0003338; L. van Waerbeke *et al.*, Astron. Astrophys. **358**, 30 (2000); D. M. Wittman, J. A. Tyson, D. Kirkman, I. Dell'Antonio, and G. Bernstein, Nature (London) **405**, 143 (2000).
[9] B. Jain and U. Seljak, Astrophys. J. **484**, 560 (1997).
[10] N. Kaiser, Astrophys. J. **498**, 26 (1998).
[11] U. Seljak, Astrophys. J. **506**, 64 (1998).
[12] W. Hu, Astrophys. J. Lett. **522**, 21 (1999).
[13] W. Hu, Phys. Rev. D **65**, 023003 (2002).
[14] W. Hu, Phys. Rev. D **66**, 083515 (2002).
[15] D. Huterer, Phys. Rev. D **65**, 063001 (2002).
[16] K. N. Abazajian and S. Dodelson, Phys. Rev. Lett. **91**, 041301 (2003).
[17] A. Heavens, arXiv:astro-ph/0304151.
[18] A. Refregier *et al.*, arXiv:astro-ph/0304419.
[19] L. Knox, arXiv:astro-ph/0304370.
[20] E. V. Linder and A. Jenkins, arXiv:astro-ph/0305286.
[21] A. N. Taylor, astro-ph/0111605.
[22] W. Hu and C. R. Keeton, Phys. Rev. D **66**, 063506 (2003).
[23] D. Wittman, J. A. Tyson, V. E. Margoniner, J. G. Cohen, and I. P. Dell'Antonio, Astrophys. J. Lett. **557**, 89 (2001).
[24] R. Moessner and B. Jain, Mon. Not. R. Astron. Soc. **294**, L18 (1998).
[25] J. Guzik and U. Seljak, Mon. Not. R. Astron. Soc. **335**, 311 (2002).
[26] G. Bernstein (private communication).
[27] A. Cooray and R. Sheth, Phys. Rep. **372**, 1 (2002).
[28] B. Jain, R. Scranton, and R. K. Sheth, arXiv:astro-ph/0304203.
[29] M. Takada and B. Jain, arXiv:astro-ph/0304034.
[30] E. V. Linder, arXiv:astro-ph/0210217.
[31] G. Bernstein and B. Jain, arXiv:astro-ph/0309332.
[32] M. Tegmark, Phys. Rev. D **66**, 103507 (2002).
[33] R. Link and M. J. Pierce, Astrophys. J. Lett. **502**, 63 (1998).
[34] G. Golse, J. P. Kneib, and G. Soucail, arXiv:astro-ph/0205357.
[35] M. Sereno, Astron. Astrophys. **393**, 757 (2002).